

Relaxation Optimized Polarization-Coherence Transfer in Ising Spin Chains

Dionisis Stefanatos* and Navin Khaneja†

*Division of Applied Sciences,
Harvard University,
Cambridge, MA 02138*

Steffen J. Glaser‡

*Institute of Organic Chemistry and Biochemistry II,
Technische Universität München, 85747 Garching, Germany*

(Dated: December 2, 2024)

Abstract

Experiments in coherent spectroscopy correspond to control of quantum-mechanical ensembles guiding them from initial to final target states. The control inputs (pulse sequences) that accomplish these transfers should be designed to minimize the effects of relaxation and to optimize the sensitivity of the experiments. For example in Nuclear Magnetic Resonance (NMR) spectroscopy, a question of fundamental importance is what is the maximum efficiency of polarization or coherence transfer between coupled spins in the presence of relaxation. Furthermore, what is the optimal pulse sequence which achieves this efficiency? This letter is a continuation of our previous work on the above problems. Here, we attempt to answer these questions for an Ising spin chain, under the presence of transverse relaxation. The methods presented in this paper are expected to find applications not only in coherent spectroscopy but also in quantum information processing.

*Electronic address: stefanat@fas.harvard.edu

†Electronic address: navin@hrl.harvard.edu; URL: <http://hrl.harvard.edu/~navin>

‡URL: <http://ocialf.org.chemie.tu-muenchen.de/glaser>

I. INTRODUCTION

The control of quantum ensembles has many applications, ranging from coherent spectroscopy to quantum information processing. In most applications involving control and manipulation of quantum phenomena, the system of interest is not isolated but interacts with its environment. This leads to the phenomenon of relaxation, which in practise results in signal loss and ultimately limits the range of applications. Manipulating quantum systems in a manner that minimizes relaxation losses poses a fundamental challenge of utmost practical importance. A premier example is the control of spin dynamics in Nuclear Magnetic Resonance (NMR) spectroscopy [1]. In structural biology, NMR spectroscopy plays an important role because it is the only technique that allows to determine the structure of biological macromolecules, such as proteins, in aqueous solution [2]. In multidimensional NMR experiments, used in protein NMR spectroscopy, transfer of coherence between coupled nuclear spins is a crucial step [2]. However, with increasing size of molecules or molecular complexes, the rotational tumbling of the molecules becomes slower and leads to increased relaxation losses [2]. When these relaxation rates become comparable to the spin-spin couplings, the efficiency of coherence transfer is considerably reduced, leading to poor sensitivity and significantly increased measurement times.

This negative effect of relaxation on the efficiency of polarization or coherence transfer gives automatically rise to some important practical (and theoretical) problems:

1. What is the theoretical upper limit for the polarization-coherence transfer efficiency in the presence of relaxation?
2. How can this theoretical upper limit be reached experimentally?

In our previous work, we answered the above questions for a two-spin 1/2 system, with Ising coupling between the spins, under the presence of transverse relaxation [3, 4] (neglecting and including cross-correlation effects, respectively) and under the presence of both longitudinal and transverse relaxation [5], using methods of optimal control theory. In this manuscript we analyze these questions for an Ising spin chain, for the case where only the transverse relaxation mechanisms are important.

The methods developed here are not restricted to NMR applications but are also useful for answering important questions in quantum information theory. It is a fundamental problem

to understand the extent to which an open quantum system can be controlled, i.e. where all the state of a quantum-mechanical system can be steered in the presence of relaxation? How much entanglement can be produced in presence of decoherence and dissipation and what is the optimal way to synthesize unitary gates in open quantum systems so as to maximize their fidelity? All these problems are related to optimal control of quantum mechanical systems in presence of relaxation.

II. DESCRIPTION OF THE SYSTEM AND STATEMENT OF THE PROBLEM

We know from elementary quantum mechanics that the density matrix of a closed quantum system evolves unitarily as ($\hbar = 1$)

$$\frac{d\rho}{dt} = -i[H(t), \rho] . \quad (1)$$

However, in most applications of quantum control, the system under study is open, i.e. interacts with its environment (also termed lattice). This undesirable interaction with an external heat bath destroys phase correlations in the quantum system and relaxes the system to its equilibrium state. The evolution is no longer unitary. In general, it is not possible to write an evolution equation in time for the density matrix of an open system. However, in many applications of interest, the lattice can be approximated as an infinite thermostat, whose own state never changes. Under this assumption, also called the Markovian approximation, it is possible to write an equation for the density matrix ρ of the system alone, the so-called master equation. The most general form of this equation is [6]

$$\frac{d\rho}{dt} = -i[H, \rho] + L(\rho) , \quad (2)$$

$$L(\rho) = \frac{1}{2} \sum_{k,l=1}^M a_{k,l} L_{F_k, F_l}(\rho) , \quad (3)$$

$$L_{F_k, F_l}(\rho) = [F_k, \rho F_l^\dagger] + [F_k \rho, F_l^\dagger] \quad (4)$$

where H is the system's Hamiltonian and generates unitary evolution. All non-unitary relaxation dynamics is accounted for by the super-operator L . The Hermitian coefficient matrix $A = \{a_{k,l}\}$ contains the information about physical relaxation parameters (lifetimes, relaxation rates) and F_k denotes operators representing various relaxation mechanisms [4].

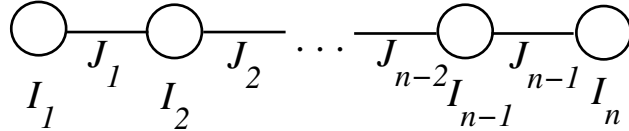


FIG. 1: The system that we study in this paper is a linear chain of n weakly interacting spins $1/2$ with Ising coupling between next neighbors. This system originates from protein NMR spectroscopy. Note that besides the coherent evolution, described by the Ising couplings, there is also dissipative evolution caused by the interaction of the system with its environment.

The system that we study in this paper originates from protein NMR spectroscopy (liquid state NMR). It is a linear chain of n weakly interacting spins $1/2$ placed in a static external magnetic field in the z direction (NMR experimental setup) and with Ising type coupling between next neighbors, see Fig. 1. In a suitably chosen (multiple) rotating frame, which rotates with each spin at its resonance (Larmor) frequency, the Hamiltonian H_f that governs the free evolution of the system is given by

$$H_f = \sum_{i=1}^{n-1} 2J_i I_{iz} I_{(i+1)z} . \quad (5)$$

Hamiltonian (5) is valid in the so-called weak coupling limit, where the resonance frequencies of the spins i and $i + 1$ satisfy $|\omega_i - \omega_{i+1}| \gg J_i$ and thus the Heisenberg coupling ($\mathbf{I}_i \cdot \mathbf{I}_{i+1}$), which is the characteristic indirect coupling between spins in isotropic liquids, can be approximated by the Ising coupling ($I_{iz} I_{(i+1)z}$) [7]. In this manuscript we examine in detail the case where the coupling constants J_i between the spins are equal. This choice simplifies the problem and is also an appropriate model for realistic situations. At the end of the paper we show how the theory can be extended to the general case of arbitrary couplings. The common coupling constant is written in the form $\sqrt{2}J$ for normalization reasons, so (5)

takes the form

$$H_f = \sqrt{2}J \sum_{i=1}^{n-1} I_{iz} I_{(i+1)z} . \quad (6)$$

About the relaxation mechanisms that contribute to the super-operator L for our system, we note that in NMR spectroscopy in liquid solutions, the most important such mechanisms are due to Dipole-Dipole (DD) interaction and Chemical Shift Anisotropy (CSA). We neglect interference effects. The corresponding relaxation operators F_k can be found in [2]. In this letter we focus on the slow tumbling regime, the so-called spin diffusion limit, which applies to biological macromolecules at high magnetic fields, where the correlation time of the molecular tumbling is much longer than the inverse of the resonance frequencies of the spins. In this limit and for DD and CSA relaxation mechanisms, as in our system, longitudinal relaxation rates (rates for operators with components only in the z direction, like $I_{iz}, 2I_{iz}I_{(i+1)z}$) are negligible compared with transverse relaxation rates (rates for operators with components in x and y directions, like $2I_{iz}I_{(i+1)x}, 2I_{iz}I_{(i+1)y}$) [8].

The problem that we address in this manuscript is to find the maximum efficiency for the polarization-coherence transfer along the spin chain

$$I_{1\alpha} \rightarrow I_{n\beta} , \quad (7)$$

where α, β can be x, y or z , under the presence of the relaxation mechanisms mentioned above. The available controls are the components ω_x and ω_y (in the rotating frame) of the transverse radiofrequency (RF) magnetic field. This comes from the NMR experimental setup. If the resonance frequencies of the spins are well separated, each spin can be selectively excited (addressed) by an appropriate choice of the components of the RF field at its resonance frequency. We want also to calculate the RF fields that maximize transfer (7).

Note that we can concentrate on the polarization transfer

$$I_{1z} \rightarrow I_{n\beta} . \quad (8)$$

Having found how to accomplish this optimally, we can use the same scheme for transfer (7). We just need to add an initial and a final 90° hard pulse to make the rotations $I_{1\alpha} \rightarrow I_{1z}, I_{1z} \rightarrow I_{n\beta}$. The way that polarization transfer (8) is done is shown in Fig. 2. From our previous work [3] we know the optimal way to do the first and the last step. In this paper

$$\begin{array}{ccccccc}
I_{1z} & \xrightarrow{\quad} & 2I_{1z} & I_{2z} & \xrightarrow{\quad} & 2I_{2z} & I_{3z} \xrightarrow{\dots} 2I_{(n-1)z} & I_{nz} \xrightarrow{\quad} & I_{nz} \\
\boxed{\quad} & & \boxed{\quad} & & & & & \boxed{\quad} & \\
\text{step 1} & & \text{step 2} & & & & & \text{step n} &
\end{array}$$

FIG. 2: Steps for the polarization transfer $I_{1z} \rightarrow I_{nz}$. From our previous work [3] we know the optimal way to do steps 1 and n, in presence of the relaxation mechanisms mentioned in the text. In this manuscript we investigate the intermediate steps. If the spins have well separated resonance frequencies, then we can selectively excite them. In this case we can examine separately each of the intermediate transfers. But the equations that describe these transfers are similar, thus we just need to study only one of them, for example the transfer $2I_{1z}I_{2z} \rightarrow 2I_{2z}I_{3z}$.

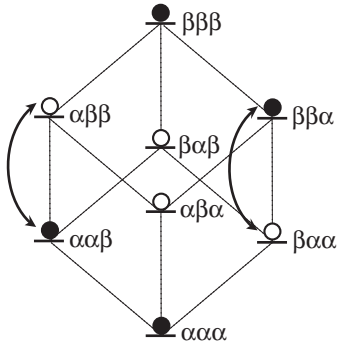


FIG. 3: Energy level diagram for a weakly coupled three-spin 1/2 chain. The dark circles indicate excess population in the corresponding levels. The selective population inversion of the levels $\alpha\alpha\beta, \alpha\beta\beta$ and $\beta\beta\alpha, \beta\alpha\alpha$ corresponds to the transfer $2I_{1z}I_{2z} \rightarrow 2I_{2z}I_{3z}$ of longitudinal two-spin order.

we investigate how can we make the intermediate steps optimally, i.e. the transfers

$$2I_{(i-1)z}I_{iz} \rightarrow 2I_{iz}I_{(i+1)z} , \quad (9)$$

where $i = 2, \dots, n-1$. Each of these transfers is done by irradiating the intermediate spin i .

If the spins have well separated frequencies, then we can selectively excite them, thus we can examine each intermediate transfer separately from the others. Additionally, the equations that describe these transfers are similar, so we actually need to study only one of them. In the following we focus on the transfer with $i = 2$

$$2I_{1z}I_{2z} \rightarrow 2I_{2z}I_{3z} . \quad (10)$$

Using the energy level diagram shown in Fig. 3, we can give a more physical picture for the full polarization transfer $I_{1z} \rightarrow I_{3z}$ along a three-spin chain. The configuration of the initial state, corresponding to polarization I_{1z} , has excess populations in the levels $\alpha\alpha\alpha, \alpha\alpha\beta, \alpha\beta\alpha, \alpha\beta\beta$ (this configuration is not shown in Fig. 3). By selectively inverting the populations of $\alpha\beta\beta, \beta\beta\beta$ and $\alpha\beta\alpha, \beta\beta\alpha$, the spin system acquires the configuration shown in Fig. 3, with excess populations in the levels $\alpha\alpha\alpha, \alpha\alpha\beta, \beta\beta\beta, \beta\beta\alpha$. This corresponds to state $2I_{1z}I_{2z}$. The next step is the selective population inversion shown in Fig. 3 ($\alpha\alpha\beta$ with $\alpha\beta\beta$ and $\beta\beta\alpha$ with $\beta\alpha\alpha$). The new configuration (excess populations in $\alpha\alpha\alpha, \alpha\beta\beta, \beta\beta\beta, \beta\alpha\alpha$) corresponds to $2I_{2z}I_{3z}$. Thus, the intermediate transfer $2I_{1z}I_{2z} \rightarrow 2I_{2z}I_{3z}$ of longitudinal two-spin order has been accomplished. The final step is to selectively invert $\alpha\beta\beta, \alpha\beta\alpha$ and $\beta\beta\beta, \beta\beta\alpha$. The final configuration (excess populations in $\alpha\alpha\alpha, \alpha\beta\alpha, \beta\alpha\alpha, \beta\beta\alpha$), not shown in Fig. 3, corresponds to polarization I_{3z} . The transfer $I_{1z} \rightarrow I_{3z}$ is completed.

III. FORMULATION OF THE PROBLEM IN TERMS OF OPTIMAL CONTROL

In this section we formulate the problem of transfer (10) in the context of optimal control. The first step is to write down evolution equations for the ensemble averages of the operators that participate in this transfer (with ensemble average of an operator O we mean $\langle O \rangle = \text{trace}\{\rho O\}$). This can be done by using the master equation (2) with the appropriate for our system H and L . The hamiltonian H is the sum of the free evolution hamiltonian H_f given in (6) and the hamiltonian H_{RF} that describes the effect of the transverse RF magnetic field. For transfer (10) only the first two terms of (6) participate, so we can set $H_f = \sqrt{2}J(I_{1z}I_{2z} + I_{2z}I_{3z})$. For the same transfer, we selectively excite only the second spin with the RF field. So $H_{RF} = \omega_x(t)I_{2x} + \omega_y(t)I_{2y}$, where ω_x, ω_y are the components of the RF field (the available controls) in the rotating frame. Using Ehrenfest's theorem we

can derive the coherent evolution of the various ensemble averages under $H = H_f + H_{RF}$. Next, we need to add the dissipative evolution caused by the relaxation term L in (2). This task is quite simple. L has no effect on the longitudinal operators $(2I_{1z}I_{2z}, 2I_{2z}I_{3z})$ since we consider the slow tumbling regime, as we mentioned above. It affects the transverse operators $(2I_{1z}I_{2x}, 2I_{2x}I_{3z})$, which relax at the same rate k . Putting all this together, we find the following system of equations (the operators appear in the order that they are produced by the coherent evolution)

$$\begin{aligned}
\frac{d}{dt}\langle 2I_{1z}I_{2z} \rangle &= \omega_x\langle 2I_{1z}I_{2y} \rangle - \omega_y\langle 2I_{1z}I_{2x} \rangle, \\
\frac{d}{dt}\langle 2I_{1z}I_{2x} \rangle &= \omega_y\langle 2I_{1z}I_{2z} \rangle - k\langle 2I_{1z}I_{2x} \rangle - J\langle \sqrt{2}(2I_{1z}I_{2y}I_{3z} + \frac{I_{2y}}{2}) \rangle, \\
\frac{d}{dt}\langle 2I_{1z}I_{2y} \rangle &= -\omega_x\langle 2I_{1z}I_{2z} \rangle - k\langle 2I_{1z}I_{2y} \rangle + J\langle \sqrt{2}(2I_{1z}I_{2x}I_{3z} + \frac{I_{2x}}{2}) \rangle, \\
\frac{d}{dt}\langle \sqrt{2}(2I_{1z}I_{2y}I_{3z} + \frac{I_{2y}}{2}) \rangle &= -\omega_x\langle \sqrt{2}(2I_{1z}I_{2z}I_{3z} + \frac{I_{2z}}{2}) \rangle + J\langle 2I_{1z}I_{2x} \rangle \\
&\quad - k\langle \sqrt{2}(2I_{1z}I_{2y}I_{3z} + \frac{I_{2y}}{2}) \rangle + J\langle 2I_{2x}I_{3z} \rangle, \\
\frac{d}{dt}\langle \sqrt{2}(2I_{1z}I_{2x}I_{3z} + \frac{I_{2x}}{2}) \rangle &= \omega_y\langle \sqrt{2}(2I_{1z}I_{2z}I_{3z} + \frac{I_{2z}}{2}) \rangle - J\langle 2I_{1z}I_{2y} \rangle \\
&\quad - k\langle \sqrt{2}(2I_{1z}I_{2x}I_{3z} + \frac{I_{2x}}{2}) \rangle - J\langle 2I_{2y}I_{3z} \rangle, \\
\frac{d}{dt}\langle \sqrt{2}(2I_{1z}I_{2z}I_{3z} + \frac{I_{2z}}{2}) \rangle &= \omega_x\langle \sqrt{2}(2I_{1z}I_{2y}I_{3z} + \frac{I_{2y}}{2}) \rangle - \omega_y\langle \sqrt{2}(2I_{1z}I_{2x}I_{3z} + \frac{I_{2x}}{2}) \rangle, \\
\frac{d}{dt}\langle 2I_{2x}I_{3z} \rangle &= \omega_y\langle 2I_{2z}I_{3z} \rangle - J\langle \sqrt{2}(2I_{1z}I_{2y}I_{3z} + \frac{I_{2y}}{2}) \rangle - k\langle 2I_{2x}I_{3z} \rangle, \\
\frac{d}{dt}\langle 2I_{2y}I_{3z} \rangle &= -\omega_x\langle 2I_{2z}I_{3z} \rangle + J\langle \sqrt{2}(2I_{1z}I_{2x}I_{3z} + \frac{I_{2x}}{2}) \rangle - k\langle 2I_{2y}I_{3z} \rangle, \\
\frac{d}{dt}\langle 2I_{2z}I_{3z} \rangle &= \omega_x\langle 2I_{2y}I_{3z} \rangle - \omega_y\langle 2I_{2x}I_{3z} \rangle.
\end{aligned}$$

We write these equations in a more clear form, to facilitate inspection. If we rescale time according to $t_{new} = Jt_{old}$ and we set

$$x_1 = \langle 2I_{1z}I_{2x} \rangle, \quad y_1 = -\langle 2I_{1z}I_{2y} \rangle, \quad z_1 = \langle 2I_{1z}I_{2z} \rangle \quad (11)$$

$$\begin{aligned}
x_2 &= \langle \sqrt{2}(2I_{1z}I_{2x}I_{3z} + \frac{I_{2x}}{2}) \rangle, \quad y_2 = \langle \sqrt{2}(2I_{1z}I_{2y}I_{3z} + \frac{I_{2y}}{2}) \rangle, \\
z_2 &= \langle \sqrt{2}(2I_{1z}I_{2z}I_{3z} + \frac{I_{2z}}{2}) \rangle
\end{aligned} \quad (12)$$

$$x_3 = -\langle 2I_{2x}I_{3z} \rangle, \quad y_3 = \langle 2I_{2y}I_{3z} \rangle, \quad z_3 = \langle 2I_{2z}I_{3z} \rangle \quad (13)$$

$$\xi = \frac{k}{J}, \quad \Omega_x = \frac{\omega_x}{J}, \quad \Omega_y = \frac{\omega_y}{J} \quad (14)$$

then the above evolution equations take the form (by abuse of notation we use the same t for the new time)

$$\dot{z}_1 = -\Omega_x y_1 - \Omega_y x_1, \quad (15)$$

$$\dot{x}_1 = \Omega_y z_1 - \xi x_1 - y_2, \quad (16)$$

$$\dot{y}_1 = \Omega_x z_1 - \xi y_1 - x_2, \quad (17)$$

$$\dot{y}_2 = -\Omega_x z_2 + x_1 - \xi y_2 - x_3, \quad (18)$$

$$\dot{x}_2 = \Omega_y z_2 + y_1 - \xi x_2 - y_3, \quad (19)$$

$$\dot{z}_2 = \Omega_x y_2 - \Omega_y x_2, \quad (20)$$

$$\dot{x}_3 = -\Omega_y z_3 - \xi x_3 + y_2, \quad (21)$$

$$\dot{y}_3 = -\Omega_x z_3 - \xi y_3 + x_2, \quad (22)$$

$$\dot{z}_3 = \Omega_x y_3 + \Omega_y x_3. \quad (23)$$

Careful inspection of equations (15)-(23) shows that there are two equivalent paths for the transfer $z_1 \rightarrow z_3$ ($2I_{1z}I_{2z} \rightarrow 2I_{2z}I_{3z}$). The first path is $z_1 \rightarrow x_1 \rightarrow y_2 \rightarrow x_3 \rightarrow z_3$ and it is encountered when $\Omega_x = 0, \Omega_y \neq 0$. The corresponding equations are (in matrix form)

$$\begin{bmatrix} \dot{z}_1 \\ \dot{x}_1 \\ \dot{y}_2 \\ \dot{x}_3 \\ \dot{z}_3 \end{bmatrix} = \begin{bmatrix} 0 & -\Omega_y & 0 & 0 & 0 \\ \Omega_y & -\xi & -1 & 0 & 0 \\ 0 & 1 & -\xi & -1 & 0 \\ 0 & 0 & 1 & -\xi & -\Omega_y \\ 0 & 0 & 0 & \Omega_y & 0 \end{bmatrix} \begin{bmatrix} z_1 \\ x_1 \\ y_2 \\ x_3 \\ z_3 \end{bmatrix} \quad (24)$$

We can shortly describe this evolution. Using the RF field Ω_y we rotate z_1 to x_1 . As we can see from the above equations, x_1 is rotated to y_2 and this to x_3 . Finally, using again Ω_y , we rotate x_3 to z_3 . The second path is $z_1 \rightarrow y_1 \rightarrow x_2 \rightarrow y_3 \rightarrow z_3$ and it is encountered when

$\Omega_x \neq 0, \Omega_y = 0$. The equations for this path are (again in matrix form)

$$\begin{bmatrix} \dot{z}_1 \\ \dot{y}_1 \\ \dot{x}_2 \\ \dot{y}_3 \\ \dot{z}_3 \end{bmatrix} = \begin{bmatrix} 0 & -\Omega_x & 0 & 0 & 0 \\ \Omega_x & -\xi & -1 & 0 & 0 \\ 0 & 1 & -\xi & -1 & 0 \\ 0 & 0 & 1 & -\xi & -\Omega_x \\ 0 & 0 & 0 & \Omega_x & 0 \end{bmatrix} \begin{bmatrix} z_1 \\ y_1 \\ x_2 \\ y_3 \\ z_3 \end{bmatrix} \quad (25)$$

Obviously, these two paths are completely equivalent.

Now let us examine what happens when both $\Omega_x, \Omega_y \neq 0$. We concentrate on path one, but the conclusions are similar for the second path. For this path, observe from (18) that when $\Omega_x \neq 0$ then y_2 is rotated to z_2 . But z_2 is not connected directly to x_3 or y_3 , which are the bridge for the final target z_3 . So, if we want to transfer z_2 to z_3 , we have to rotate it back to x_2 or y_2 . Thus, building z_2 is not useful at all. We can avoid it by using only $\Omega_y \neq 0$ or $\Omega_x \neq 0$. Each choice corresponds to one of the two paths, which are completely equivalent. We choose path one, so $\Omega_x = 0$ and $\Omega_y \neq 0$. Our goal is to find that $\Omega_y(t)$ which maximizes the transfer $z_1 \rightarrow z_3$ for the evolution equation (24), starting from the point $(z_1, x_1, y_2, x_3, z_3) = (1, 0, 0, 0, 0)$. We would also like to find the maximum achievable value of z_3 .

IV. CONVENTIONAL APPROACH AND COMMENTS ON THE OPTIMAL CONTROL PROBLEM

The conventional method used for doing this transfer is the INEPT (Insensitive Nuclei Enhanced by Polarization Transfer) pulse sequence. We describe it briefly. At time $t = 0^-$ we apply a 90° hard pulse in the y direction, which rotates instantaneously z_1 to x_1 . The initial condition for x_1 changes from $x_1(0^-) = 0$ to $x_1(0^+) = 1$. Next, we let the system evolve freely. As we can see from (24), this evolution is governed by the equations

$$\begin{bmatrix} \dot{x}_1 \\ \dot{y}_2 \\ \dot{x}_3 \end{bmatrix} = \begin{bmatrix} -\xi & -1 & 0 \\ 1 & -\xi & -1 \\ 0 & 1 & -\xi \end{bmatrix} \begin{bmatrix} x_1 \\ y_2 \\ x_3 \end{bmatrix} \quad (26)$$

Using the initial condition $(x_1, y_2, x_3) = (1, 0, 0)$, we find that

$$x_3(t) = \frac{1}{2}e^{-\xi t}[1 - \cos(\sqrt{2}t)]. \quad (27)$$

The value of x_3 is maximized at the time $t = t_m$ which satisfies

$$\frac{dx_3}{dt} \Big|_{t=t_m} = 0 \quad \Rightarrow \quad \sin(\sqrt{2}t_m) = \xi[1 - \cos(\sqrt{2}t_m)] \quad (28)$$

At time $t = t_m^-$ we apply a second 90° hard pulse in the y direction, which rotates instantaneously x_3 to z_3 . The INEPT pulse sequence is completed and the transfer efficiency is

$$\eta_I = z_3(t_m^+) = x_3(t_m^-) = \frac{1}{2}e^{-\xi t_m}[1 - \cos(\sqrt{2}t_m)], \quad (29)$$

where t_m is calculated from (28).

The basic idea of our approach to the problem is to use the RF field $\Omega_y(t)$ to rotate gradually z_1 to x_1 and x_3 to z_3 , instead of using hard pulses. This method is better than the conventional one presented above. We can explain this using the system equation (24). Suppose that the available time T for the application of the RF field is specified. If we choose $\Omega_y(t)$ to make the rotations $z_1 \rightarrow x_1$, $x_3 \rightarrow z_3$ fast enough, like in the conventional method, the intermediate transverse variables x_1 , y_2 and x_3 are built quickly. As we can observe from (24), these variables are exposed to the phenomenon of relaxation which limits the performance. But if we choose $\Omega_y(t)$ to make these rotations in the appropriate rate, then we can accomplish the desired transfer by building the intermediate transverse variables gradually, thus reducing the relaxation losses. For more details about how we can exploit gradual rotations (instead of using hard pulses) to improve the efficiency of a system limited by relaxation, we refer to [3], [5].

The maximum achievable value of z_3 corresponds to the limiting case where the duration T of the experiment approaches infinity. This can be easily proved. Suppose that we have two available times T_1 and T_2 , with $T_1 < T_2$. Suppose also that we have found an optimal policy P_1 (the optimal control $\Omega_y(t)$) for the time interval $[0, T_1]$, which gives us a transfer efficiency $z_3(T_1) = \eta_1$. For the available time T_2 , if we apply the policy P_1 for $t \in [0, T_1]$ and then set $\Omega_y(t) = 0$ for $t \in (T_1, T_2]$, we get the same efficiency η_1 . Of course, we can find an optimal policy P_2 for the whole time interval $[0, T_2]$. Let η_2 be the transfer efficiency under this policy. Obviously it is $\eta_2 \geq \eta_1$. Thus the longer the available time the better efficiency we may get. The physical explanation is that the longitudinal (z) direction is protected against relaxation. The maximum transfer efficiency is achieved in the limiting case where the available time approaches infinity. In control language, we need to consider our problem as an *infinite horizon problem*.

Finding an analytic solution for this optimal control problem is not an easy task. The difficulty comes from the fact that the control Hamiltonian for system (24) is linear in the control variable Ω_y and, additionally, this variable is unbounded. Nevertheless, we can transform our problem to another one which can be solved analytically if we ignore some specific constraints, thus establishing an analytic upper bound for the maximum achievable value of z_3 . This is the subject of the following section.

V. AN UPPER BOUND FOR THE EFFICIENCY

We mentioned above that it is not easy to find an analytic solution for the optimal control problem, since the corresponding control Hamiltonian is linear in Ω_y . We can overcome this obstacle by a suitable transformation. This transformation treats the linearity problem but creates another one. Nevertheless, we can use the resulting system to derive an analytic upper bound for the efficiency achievable by the original system (24).

Define

$$r_1 = \sqrt{z_1^2 + x_1^2}, \quad r_2 = y_2, \quad r_3 = \sqrt{z_3^2 + x_3^2}. \quad (30)$$

Using the RF field Ω_y we can control the angles θ_1, θ_3 shown in Fig. 4. So, instead of Ω_y , we can use as control parameters the cosines of these angles $u_1 = \cos \theta_1 = x_1/r_1, u_3 = \cos \theta_3 = x_3/r_3$, where $0 \leq u_1, u_3 \leq 1$. If we use equation (24) and the previous definitions for u_1, u_3 ,

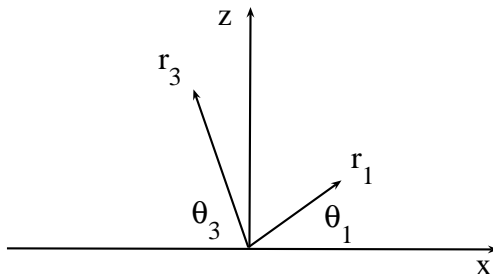


FIG. 4: Using the RF field Ω_y we can control the angles θ_1, θ_3 .

we find the following system for r_i , $i = 1, 2, 3$:

$$\begin{bmatrix} \dot{r}_1 \\ \dot{r}_2 \\ \dot{r}_3 \end{bmatrix} = \begin{bmatrix} -\xi u_1^2 & -u_1 & 0 \\ u_1 & -\xi & -u_3 \\ 0 & u_3 & -\xi u_3^2 \end{bmatrix} \begin{bmatrix} r_1 \\ r_2 \\ r_3 \end{bmatrix} \quad (31)$$

The initial problem has been transformed to the following: given the dynamical system above, we want to find the optimal values of $u_1(t)$ and $u_3(t)$, so that starting from $(r_1(0), r_2(0), r_3(0)) = (1, 0, 0)$ we achieve the largest value of r_3 . But there is an important limitation for using system (31) instead of the original one. The control parameters u_1 and u_3 are not independent, since the angles θ_1, θ_3 are both controlled by Ω_y , see Fig. 4. Nevertheless, we can still exploit system (31). If we consider u_1, u_3 independent and find the transfer efficiency, this is an upper bound for the efficiency of the original problem. In the following, we solve the infinite horizon problem for system (31), considering u_1, u_3 independent. Note that for this system the control Hamiltonian is quadratic in u_1, u_3 , so the use of analytic optimization methods is possible. Here, we do not give a strict mathematical proof but a more 'physical' one. The formal mathematical proof can be found in [9].

As r_1 is transferred to r_3 , the ratio r_3/r_1 increases from 0 to ∞ . The optimal choice of u_1 and u_3 must ensure that the ratio of gain dr_3 in r_3 to loss dr_1 in r_1 for incremental time steps dt is maximized at each step. This ratio is (use equation (31) and that $\dot{r}_1 < 0, \dot{r}_3 > 0$)

$$\frac{|\dot{r}_3|}{|\dot{r}_1|} = \frac{u_3 r_2 - \xi u_3^2 r_3}{\xi u_1^2 r_1 + u_1 r_2} \quad (32)$$

Let

$$\frac{u_1 r_1}{r_2} = p, \quad \frac{u_3 r_3}{r_2} = q \quad (33)$$

Then, equation (32) becomes

$$\frac{|\dot{r}_3|}{|\dot{r}_1|} = \frac{r_1 q - \xi q^2}{r_3 \xi p^2 + p} \quad (34)$$

We want to maximize this expression with respect to p and q . So, we just need to maximize the function

$$f(p, q) = \frac{q - \xi q^2}{\xi p^2 + p} \quad (35)$$

The first idea is to take the derivatives of f with respect to p, q and set them equal to zero. But we have to be careful because p and q are related in some way. Up to now he have

used the system equations for r_1 and r_3 . What about the equation for r_2 ? What kind of information can we extract from this? Using the equation for r_2 from (31), we easily find

$$\frac{d}{dt} \left(\frac{1}{2} r_2^2 \right) = u_1 r_1 r_2 - \xi r_2^2 - r_2 u_3 r_3 , \quad (36)$$

or, using (33)

$$\frac{d}{dt} \left(\frac{1}{2} r_2^2 \right) = (p - \xi - q) r_2^2 \quad (37)$$

Note that if we start from $r_2(0) = 0$, then r_2 remains zero and there is no evolution from r_1 to r_3 (observe from (31) that r_1, r_3 are not directly related but they are connected through r_2). What really happens is that we have to start the system from a small positive value of $r_2(0) = \epsilon > 0$. As far as the available time is infinite, ϵ can be chosen arbitrarily small. With this initial condition, equation (37) gives

$$r_2(t) = \epsilon e^{-kt}, \quad (38)$$

where

$$k = \xi + q - p . \quad (39)$$

In the optimal case, r_2 should not increase with time (remember that we want to get the maximum r_3), so it must be $k \geq 0$. Then, the necessary time for the transfer $r_1 \rightarrow r_3$ through $r_2 = \epsilon e^{-kt}$ is roughly speaking $\sim 1/\epsilon$. This implies that the optimal rate constant k should be $k \sim \epsilon$. In the limit $\epsilon \rightarrow 0$, k should also tend to zero. So the optimal choice is $k = 0$. Observe that in this case $\dot{r}_2 = 0$, thus r_2 remains constant throughout. The transfer $r_1 \rightarrow r_3$ is done adiabatically through the infinitesimal $r_2 = \epsilon$. Since $k = 0 \Rightarrow p = \xi + q$, f becomes a simple function of $q > 0$

$$g(q) = f(\xi + q, q) = \frac{q - \xi q^2}{\xi(\xi + q)^2 + \xi + q} \quad (40)$$

This function achieves its maximum for $dg/dq = 0$. Using this, we can calculate q_{opt} as a function of ξ . Then, we use the relation $p = \xi + q$ to calculate p_{opt} . We find

$$p_{opt} = \frac{\xi + \sqrt{\xi^2 + 2}}{2}, \quad q_{opt} = \frac{-\xi + \sqrt{\xi^2 + 2}}{2} \quad (41)$$

The optimal choice of u_1, u_3 satisfies

$$\frac{u_1 r_1}{r_2} = p_{opt}, \quad \frac{u_3 r_3}{r_2} = q_{opt} \quad (42)$$

The corresponding maximum value of f is

$$f_{max} = f(p_{opt}, q_{opt}) = \frac{(\sqrt{\xi^2 + 2} - \xi)^4}{4} \quad (43)$$

Using (34), (35) and that $\dot{r}_1 < 0, \dot{r}_3 > 0$, we find that for the optimal choice of u_1, u_3 it is

$$r_3^2 + f_{max}r_1^2 = \text{constant} \quad (44)$$

But $r_1(0) = 1, r_3(0) = 0$, so the above relation becomes

$$r_3^2 + f_{max}r_1^2 = f_{max} \quad (45)$$

As $t \rightarrow \infty, r_1 \rightarrow 0$. Thus

$$r_3(t \rightarrow \infty) \rightarrow \sqrt{f_{max}} = \frac{(\sqrt{\xi^2 + 2} - \xi)^2}{2} \equiv v. \quad (46)$$

This is the maximum efficiency for the transfer $r_1 \rightarrow r_3$ when we take u_1, u_3 independent. Note also that the fulfilment of optimal conditions (42) requires that at some times the restrictions $0 \leq u_1, u_3 \leq 1$ are violated. Thus v in (46) is an upper bound for the efficiency of the transformed form of the original problem, where u_1, u_3 are no longer independent and, additionally, $0 \leq u_1, u_3 \leq 1$. We emphasize that we cannot achieve v using the real system (24). What we can do is to calculate numerically, for each value of ξ , a RF field Ω_y that, when applied to the real system (24), gives a value of z_3 approaching this upper bound. This is the subject of section VI.

VI. NUMERICAL CALCULATION OF THE OPTIMAL RF FIELD

Having established an analytical upper bound (46) for the efficiency, we now try to find numerically a RF field $\Omega_y(t)$ that approaches this bound, for each value of the parameter ξ . The methods that we employ in this section use the equations (24) of the original system.

At first, we use a numerical optimization method based on a steepest descent algorithm. For the application of the method we use a finite time window T , although the maximum efficiency is achieved for $T \rightarrow \infty$, as mentioned above. Using a big enough T is sufficient, since the major improvement in the efficiency by the use of gradual rotations for systems with only transverse relaxation present is achieved for finite times, see for example [3]. For the values of normalized relaxation ξ that we are interested in $(0 - 1)$, a time interval $T = 10$

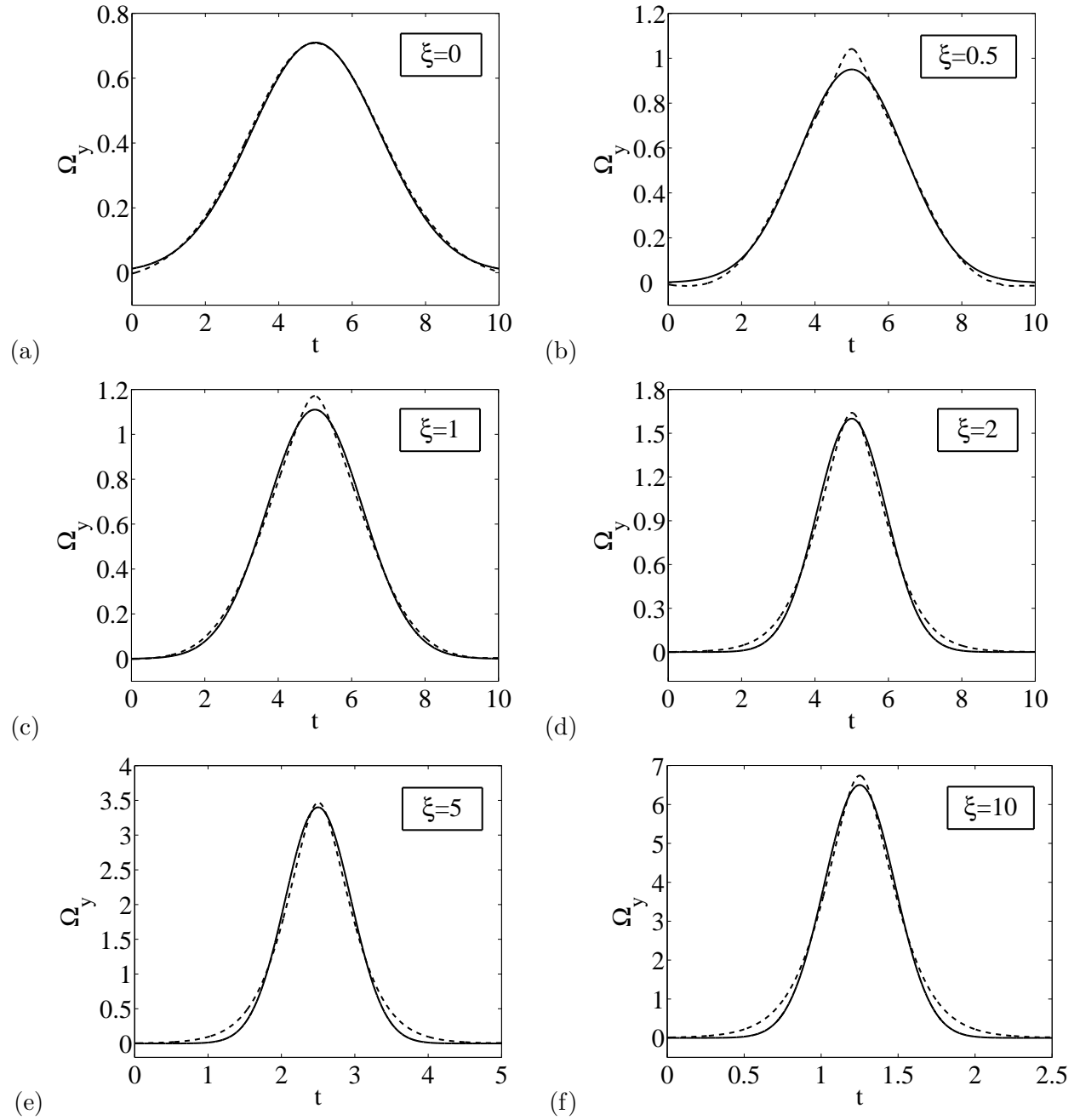


FIG. 5: Optimal pulse (dashed line) calculated using a numerical optimization method based on a steepest descent algorithm, for various values of the normalized relaxation parameter ξ . The Gaussian pulse (solid line) approximates very well the optimal pulse shape and gives a similar efficiency. This suggests that instead of using the initial numerical optimization method, we can use Gaussian pulses of the form (47), optimized with respect to A and σ for each value of ξ .

(normalized time units) is enough. For larger values of ξ we can use even shorter T . The optimal RF field $\Omega_y(t)$ that we find with this method, for various ξ , is shown in Fig. 5. Note that as ξ increases, the optimal pulse, calculated for a fixed time window, becomes shorter in time and acquires a larger peak value. The reason for this is that when the available time is finite, then the transfer $z_1 \rightarrow z_3$ should be done faster for larger ξ , in order to reduce the increased relaxation losses. Now observe that the optimal pulse shape can be very well approximated by a Gaussian profile of the form

$$\Omega_y(t) = A \exp \left[\left(\frac{t - T/2}{\sqrt{2}\sigma} \right)^2 \right], \quad (47)$$

with A, σ appropriately chosen. As a result, the efficiency that we find using the appropriate Gaussian pulse is very close to that we find using the original pulse. This suggests that instead of using the initial numerical optimization method, we can use Gaussian pulses of the form (47), optimized with respect to A and σ for each value of ξ . The optimal A, σ are found by numerical simulations. For each ξ we simulate the equations of system (24) with $\Omega_y(t)$ given by (47), for many values of A and σ . We choose those values that give the maximum $z_3(T)$. In Table I we show the optimal A, σ , for various values $\xi \in [0, 1]$. We also show the corresponding efficiency, as well as the efficiency achieved by the initial numerical optimization method. Observe how close lie these two groups of values, especially for large relaxation rates ($\xi > 0.5$). The choice of the Gaussian shape is indeed successful.

Fig. 6 shows the efficiency of the conventional method (INEPT), the efficiency of our method (SPORTS ROPE, SPin ORder TranSfer with Relaxation Optimized Pulse Element) and the upper bound v from (46), for the values of the relaxation parameter ξ shown in Table I. Note that for large ξ (large relaxation rates), SPORTS ROPE gives a significant improvement over INEPT.

In Fig. 7(a) we plot the time evolution of the various transfer functions (operators) that participate in the transfer $z_1 \rightarrow z_3$, when the optimal Gaussian pulse for $\xi = 1$, shown in Fig. 5(c), is applied to system (24). Observe the gradual building of the intermediate variables x_1, y_2 and x_3 . In Fig. 7(b) we plot the angle $\theta_3 = \tan^{-1}(z_3/x_3)$ of the vector $\mathbf{r}_3 = x_3\hat{x} + z_3\hat{z}$ with the x axis, as a function of time. Observe that initially \mathbf{r}_3 is parallel to x axis ($\theta = 0$), but under the action of the Gaussian pulse is rotated gradually to z axis ($\theta = \pi/2$). The gradual rotation of x_3 to z_3 is the spirit of SPORTS ROPE.

We remark that for the general transfer $I_{1z} \rightarrow I_{nz}$, more than one intermediate steps

TABLE I: For various values of $\xi \in [0, 1]$, the optimal values of A , σ and the corresponding efficiency are shown. We present also for comparison the efficiency achieved by the steepest descent method.

ξ	A	σ	Gaussian Pulse	Steepest Descent
1.00	1.11	1.30	0.2510	0.2512
0.95	1.09	1.32	0.2661	0.2662
0.90	1.07	1.34	0.2824	0.2825
0.85	1.05	1.36	0.3000	0.3001
0.80	1.03	1.38	0.3190	0.3191
0.75	1.02	1.39	0.3396	0.3397
0.70	1.00	1.41	0.3619	0.3620
0.65	0.98	1.43	0.3861	0.3863
0.60	0.97	1.44	0.4124	0.4126
0.55	0.96	1.44	0.4410	0.4413
0.50	0.95	1.44	0.4721	0.4726
0.45	0.94	1.45	0.5060	0.5067
0.40	0.93	1.46	0.5428	0.5439
0.35	0.92	1.46	0.5830	0.5846
0.30	0.91	1.46	0.6270	0.6292
0.25	0.90	1.47	0.6750	0.6780
0.20	0.89	1.48	0.7277	0.7315
0.15	0.88	1.48	0.7855	0.7900
0.10	0.85	1.52	0.8494	0.8536
0.05	0.79	1.60	0.9203	0.9232
0.00	0.73	1.71	0.9999	1.0000

$2I_{(i-1)z}I_{iz} \rightarrow 2I_{iz}I_{(i+1)z}$ are necessary. Since the equations that describe the i^{th} transfer are the same as (24), we just need to apply the same Gaussian pulse but centered, in the frequency domain, at the resonance frequency of spin i . In this sequence of Gaussian pulses we should add at the beginning and at the end the optimal pulses for the first and the final step, respectively, see Fig. 2. These pulses can be calculated using the theory presented in

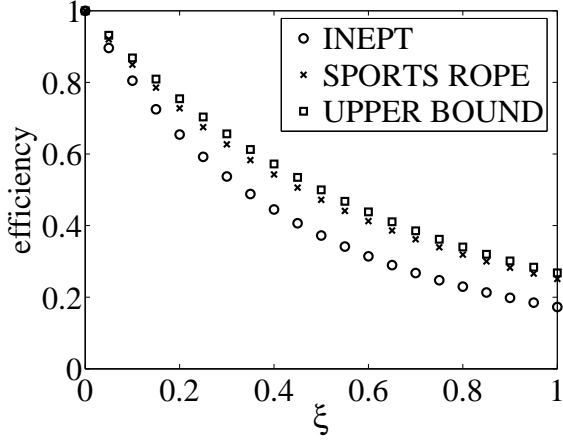


FIG. 6: Efficiency for the conventional method (INEPT) and for our method (SPORTS ROPE), for the values of ξ shown in Table I. We also plot the upper bound (46) for the efficiency.

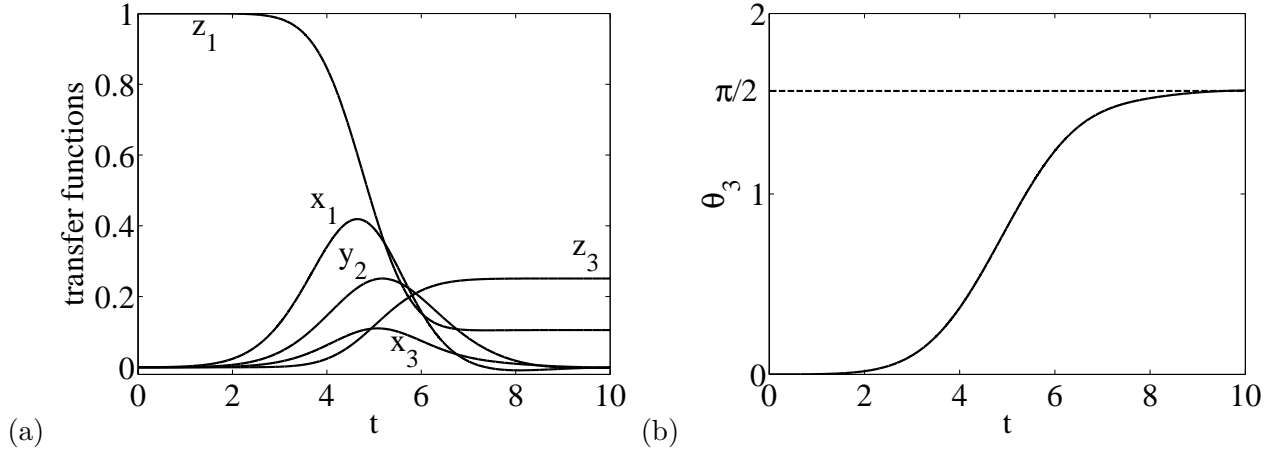


FIG. 7: (a) Time evolution of the transfer functions (operators) that participate in the transfer $z_1 \rightarrow z_3$, for $\xi = 1$ and the optimal Gaussian pulse shown in Fig. 5(c) (b) The angle $\theta_3 = \tan^{-1}(z_3/x_3)$ of the vector $\mathbf{r}_3 = x_3\hat{x} + z_3\hat{z}$ with the x axis, as a function of time. Observe that initially \mathbf{r}_3 is parallel to x axis ($\theta = 0$), but under the action of the Gaussian pulse is rotated gradually to z axis ($\theta = \pi/2$).

[3].

VII. THE GENERAL CASE WITH ARBITRARY COUPLING CONSTANTS

In this section we study transfer (10) but for the general form of the free evolution Hamiltonian H_f

$$H_f = 2J_1 I_{1z} I_{2z} + 2J_2 I_{2z} I_{3z} . \quad (48)$$

If we work as in section III with $H = H_f + H_{rf}$, $H_{rf} = \omega_x I_{2x} + \omega_y I_{2y}$, we can derive evolution equations for the average values of the various operators participating in the transfer. Again, two equivalent paths can be identified in the resulting set of equations: One with $\Omega_x = 0, \Omega_y \neq 0$ and one with $\Omega_x \neq 0, \Omega_y = 0$. As before, we just need to consider only one of them, for example the first path. The corresponding equations in matrix form are

$$\begin{bmatrix} \dot{z}_1 \\ \dot{x}_1 \\ \dot{y}_2 \\ \dot{y}_3 \\ \dot{x}_4 \\ \dot{z}_4 \end{bmatrix} = \begin{bmatrix} 0 & -\Omega_y & 0 & 0 & 0 & 0 \\ \Omega_y & -1 & -\zeta_1 & -\zeta_2 & 0 & 0 \\ 0 & \zeta_1 & -1 & 0 & -\zeta_2 & 0 \\ 0 & \zeta_2 & 0 & -1 & -\zeta_1 & 0 \\ 0 & 0 & \zeta_2 & \zeta_1 & -1 & -\Omega_y \\ 0 & 0 & 0 & 0 & \Omega_y & 0 \end{bmatrix} \begin{bmatrix} z_1 \\ x_1 \\ y_2 \\ y_3 \\ x_4 \\ z_4 \end{bmatrix} , \quad (49)$$

where

$$x_1 = \langle 2I_{1z} I_{2x} \rangle, \quad z_1 = \langle 2I_{1z} I_{2z} \rangle , \quad (50)$$

$$y_2 = \langle I_{2y} \rangle, \quad y_3 = \langle 4I_{1z} I_{2y} I_{3z} \rangle , \quad (51)$$

$$x_4 = -\langle 2I_{2x} I_{3z} \rangle, \quad z_4 = \langle 2I_{2z} I_{3z} \rangle , \quad (52)$$

$$\zeta_1 = \frac{J_1}{k}, \quad \zeta_2 = \frac{J_2}{k}, \quad \Omega_y = \frac{\omega_y}{k} . \quad (53)$$

Note that in system (49) there is one more equation than in system (24). This happens because the term $y_2 = \langle \sqrt{2}(2I_{1z} I_{2y} I_{3z} + I_{2y}/2) \rangle$ in (24) splits into two terms, $y_2 = \langle I_{2y} \rangle$ and $y_3 = \langle 4I_{1z} I_{2y} I_{3z} \rangle$ in (49), which evolve differently for $\zeta_1 \neq \zeta_2$.

An upper bound for the maximum achievable value of z_4 , starting from $(z_1, x_1, y_2, y_3, x_4, z_4) = (1, 0, 0, 0, 0, 0)$, can be found by using the theory presented in [9]. Consider the system

$$\begin{bmatrix} \dot{z}_1 \\ \dot{z}_2 \\ \dot{z}_3 \\ \dot{z}_4 \\ \dot{x}_1 \\ \dot{y}_2 \\ \dot{y}_3 \\ \dot{x}_4 \end{bmatrix} = \begin{bmatrix} 0 & 0 & 0 & 0 & -v_1 & 0 & 0 & 0 \\ 0 & 0 & 0 & 0 & 0 & -v_2 & 0 & 0 \\ 0 & 0 & 0 & 0 & 0 & 0 & -v_3 & 0 \\ 0 & 0 & 0 & 0 & 0 & 0 & 0 & -v_4 \\ v_1 & 0 & 0 & 0 & -1 & -\zeta_1 & -\zeta_2 & 0 \\ 0 & v_2 & 0 & 0 & \zeta_1 & -1 & 0 & -\zeta_2 \\ 0 & 0 & v_3 & 0 & \zeta_2 & 0 & -1 & -\zeta_1 \\ 0 & 0 & 0 & v_4 & 0 & \zeta_2 & \zeta_1 & -1 \end{bmatrix} \begin{bmatrix} z_1 \\ z_2 \\ z_3 \\ z_4 \\ x_1 \\ y_2 \\ y_3 \\ x_4 \end{bmatrix}, \quad (54)$$

Observe that system (54) reduces to system (49) for $v_1 = -v_4 = \Omega_y, v_2 = v_3 = 0$. Thus, if we know the maximum achievable value of z_4 starting from $(1, 0, 0, 0, 0, 0, 0, 0)$ and evolving under system (54), then this is an upper bound for the maximum achievable value of z_4 with evolution described by the original system (49). In [9] we show that the maximum efficiency for systems like (54) can be found by solving an appropriate semidefinite program. Semidefinite programming is a branch of convex optimization, with many applications in engineering [10]. We describe the semidefinite program that we need to solve for the particular case that we examine. Let us define the inner product $\langle \cdot, \cdot \rangle$ of two symmetric matrices A, B as the trace of their matrix product, $\langle A, B \rangle = \text{tr}(AB)$. We also define the following matrices

$$A_1 = \begin{bmatrix} -2 & -\zeta_1 & -\zeta_2 & 0 \\ -\zeta_1 & 0 & 0 & 0 \\ -\zeta_2 & 0 & 0 & 0 \\ 0 & 0 & 0 & 0 \end{bmatrix}, \quad A_2 = \begin{bmatrix} 0 & \zeta_1 & 0 & 0 \\ \zeta_1 & -2 & 0 & -\zeta_2 \\ 0 & 0 & 0 & 0 \\ 0 & -\zeta_2 & 0 & 0 \end{bmatrix},$$

$$A_3 = \begin{bmatrix} 0 & 0 & \zeta_2 & 0 \\ 0 & 0 & 0 & 0 \\ \zeta_2 & 0 & -2 & -\zeta_1 \\ 0 & 0 & -\zeta_1 & 0 \end{bmatrix}, \quad A_4 = \begin{bmatrix} 0 & 0 & 0 & 0 \\ 0 & 0 & 0 & \zeta_2 \\ 0 & 0 & 0 & \zeta_1 \\ 0 & \zeta_2 & \zeta_1 & -2 \end{bmatrix}.$$

Using the theory developed in [9], we easily see that the semidefinite program of interest is the following: Find

$$\mathcal{E} = \max_M \langle A_n, M \rangle$$

subject to

$$\langle A_1, M \rangle = -1, \quad \langle A_2, M \rangle = 0, \quad \langle A_3, M \rangle = 0$$

and M positive semidefinite symmetric 4×4 matrix. The maximum achievable value of z_4 for system (54) is $v = \sqrt{\mathcal{E}}$ and this is an upper bound for the corresponding value for system (49).

This semidefinite program can be solved by using some appropriate software package, for example SDPT3, [11]. As an illustration, we consider the case $J_1 = J_2 = k/\sqrt{2}$ ($\zeta_1 = \zeta_2 = 1/\sqrt{2}$). This corresponds to $J = k$ ($\xi = 1$) for system (24). We find $\mathcal{E} = 0.0718 \Rightarrow v = \sqrt{\mathcal{E}} = 0.2679$. On the other hand, using formula (46) with $\xi = 1$ we find $v = 0.2679$, i.e. the same value. Calculating numerically the upper bound for various values of ζ_1 and ζ_2 , leads us to the following very important observation. If we keep ζ_2 fixed and calculate the upper bound v for increasing values of ζ_1 , we find that after some point the further increase of ζ_1 has no effect to the value of v . This is shown in Table II.

TABLE II: For $\zeta_2 = 0.5$ fixed we have calculated the upper bound v for increasing values of ζ_1 . Observe that after $\zeta_1 = 1.5$, v becomes insensitive in the further increase of ζ_1 .

ζ_1	0.5	0.6	0.7	0.8	0.9	1	1.5	2	2.5
ζ_2	0.5	0.5	0.5	0.5	0.5	0.5	0.5	0.5	0.5
v	0.1715	0.1934	0.2100	0.2220	0.2300	0.2345	0.2360	0.2360	0.2360

For the general case $J_1 \neq J_2$ and working analogously with the case $J_1 = J_2 = J$, we can calculate the efficiency accomplished by the conventional method, INEPT. We can also use a steepest descent algorithm to calculate numerically the optimal pulse $\Omega_y(t)$ and compare the efficiency achieved with the upper bound obtained by solving the corresponding semidefinite program. About the optimal pulse shape, we find after numerical investigation that if the values of ζ_1 and ζ_2 are relatively close to each other then again it can be very well approximated by a Gaussian profile of the form (47). Otherwise, if ζ_1 is much different than ζ_2 , the optimal pulse shape is more complicated. It develops wings and we have to use more complicated profiles to approximate it, for example the Mexican hat profile

$$\Omega_y(t) = A \left[1 - \left(\frac{t - T/2}{b} \right)^2 \right] \exp \left[- \left(\frac{t - T/2}{\sqrt{2}\sigma} \right)^2 \right]. \quad (55)$$

For $J_1 = k$, $J_2 = 0.5k$ ($\zeta_1 = 1$, $\zeta_2 = 0.5$) the Gaussian profile is a good approximation to the optimal pulse shape. In Fig. 8(a) we plot the optimal Gaussian pulse and in Fig. 8(b) the time evolution of the various transfer functions under this pulse. For $J_1 = 2k$, $J_2 = 0.5k$ ($\zeta_1 = 2$, $\zeta_2 = 0.5$) the optimal pulse shape is more complicated and a Mexican hat profile gives a better approximation than a Gaussian. The optimal Mexican hat pulse is shown in Fig. 9(a) and the corresponding evolution of the transfer functions in Fig. 9(b). Note that for both cases function y_3 is developed less than function y_2 . This happens because y_3 is connected to x_1 by the smallest coupling ζ_2 while is connected to x_4 by the largest coupling ζ_1 . As a result, y_3 is built less and depleted faster, that's why is developed less than y_2 in the course of time. If the couplings were equal, then y_2 and y_3 would have the same time evolution and if $\zeta_1 < \zeta_2$ then y_3 would be developed more than y_2 . In Table III we show the values of the parameters (A , σ and b) used for the two cases, the efficiency achieved by the conventional method (INEPT), our method (SPORTS ROPE), and the upper bound calculated using semidefinite programming. Note that although the efficiency of SPORTS ROPE and the upper bound are pretty much the same for the two cases (see the observation in the preceding paragraph), the efficiency of INEPT is different. It is larger for the second case, because INEPT exploits better the larger ζ_1 .

We conclude this chapter by noting that the general method for calculating efficiency upper bounds, using semidefinite programming, can be extended to the more general case where interference phenomena between the various relaxation mechanisms are taken into account.

- [1] R.R. Ernst, G. Bodenhausen, A. Wokaun, *Principles of Nuclear Magnetic Resonance in One and Two Dimensions* (Clarendon Press, Oxford, 1987).
- [2] J. Cavanagh, W.J. Fairbrother, A.G. Palmer III, and N.J. Skelton, *Protein NMR Spectroscopy* (Academic Press, New York, 1996).
- [3] N. Khaneja, T. Reiss, B. Luy, and S.J. Glaser, *J. Magn. Reson.* 162, 311 (2003).
- [4] N. Khaneja, B. Luy, and S.J. Glaser, *Proc. Natl. Acad. Sci. U.S.A.* 100, 13162 (2003).
- [5] D. Stefanatos, N. Khaneja, and S.J. Glaser, *Phys. Rev. A* 69, 022319 (2004).
- [6] R. Alicki, K. Lendi, *Quantum Dynamical Semigroups and Applications*, Lecture Notes in

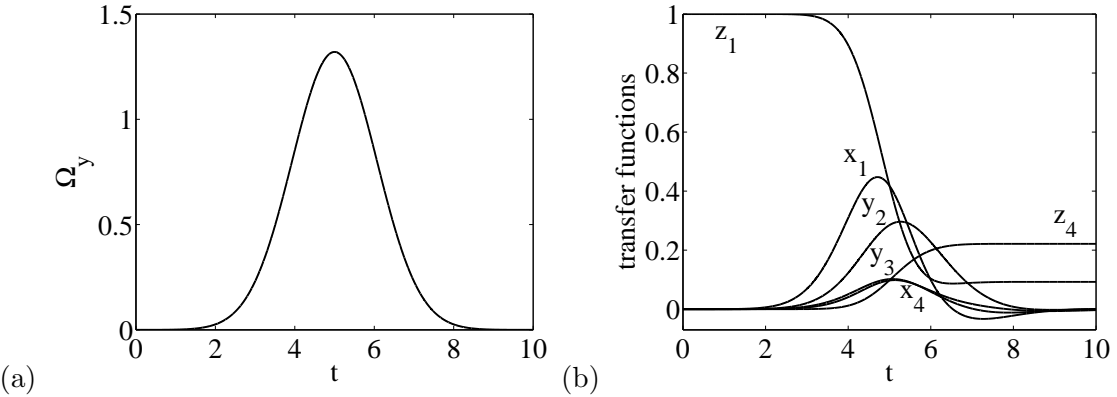


FIG. 8: (a) The Gaussian pulse that approximates the optimal pulse shape for $J_1 = k, J_2 = 0.5k$ ($\zeta_1 = 1, \zeta_2 = 0.5$) (b) The corresponding time evolution of the transfer functions. Note that y_3 and x_4 have a similar time evolution.

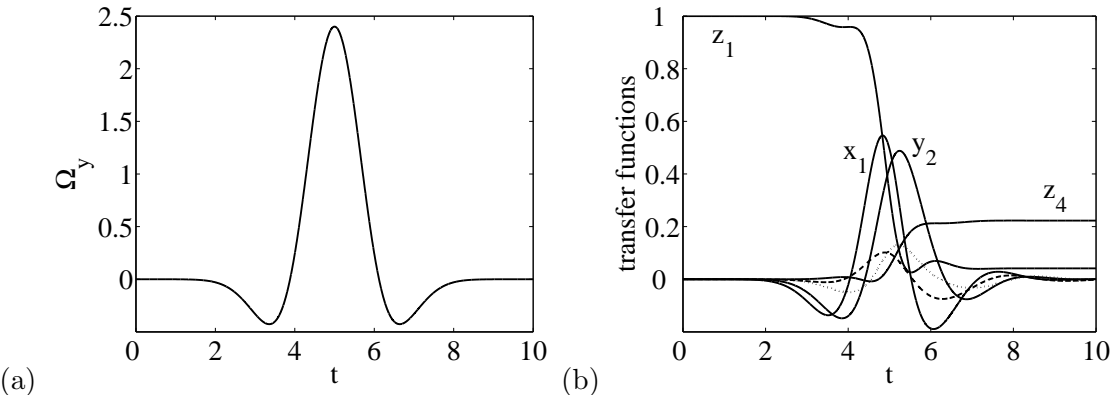


FIG. 9: (a) The Mexican hat pulse that approximates the optimal pulse shape for $J_1 = 2k, J_2 = 0.5k$ ($\zeta_1 = 2, \zeta_2 = 0.5$) (b) Time evolution of the corresponding transfer functions. Note that the dashed line corresponds to y_3 while the dotted line to x_4 .

TABLE III: For the two cases with $J_1 \neq J_2$ examined in the text, we show the optimal values of A, σ, b , the efficiency achieved by the conventional method (INEPT), our method (SPORTS ROPE), and the upper bound calculated using semidefinite programming.

ζ_1	ζ_2	A	σ	b	INEPT	SPORTS ROPE	Upper Bound
1.0	0.5	1.32	1.07	-	0.1593	0.2214	0.2345
2.0	0.5	2.40	0.85	1.12	0.1755	0.2230	0.2360

Physics, Springer, Berlin, Vol. 286, 1987

- [7] M. H. Levitt, Spin Dynamics (John Wiley and Sons, New York, 2001).
- [8] M. Goldman, J. Magn. Reson. 60, 437 (1984).
- [9] D. Stefanatos and N. Khaneja, e-print math.OC/0504308
- [10] L. Vandenberghe and S. Boyd, SIAM Review 38(1), 49 (1996).
- [11] K. C. Toh, M. J. Todd and R. H. Tütüncü, Optimization Methods and Software 11, 545 (1999).